Factors suppressing transport critical current in Ag/Bi2223 tapes

K. Osamura,[a] S. Nonaka, M. Matsui, and T. Oku
Department of Materials Science and Engineering, Kyoto University, Sakyo-ku, Kyoto 606-01, Japan

S. Ochiai
Mesoscopic Materials Research Center, Kyoto University, Sakyo-ku, Kyoto, 606-01, Japan

D. P. Hampshire
Department of Physics, University of Durham, South Road, Durham DH1 3LE, United Kingdom

(Received 9 November 1995; accepted for publication 7 February 1996)

The microstructural factors limiting the critical current density J_c have been investigated for the silver-sheathed Bi2223 tapes prepared by the powder-in-tube technique. In a hierarchy among them, which factor is the most effective in determining J_c depends on how extensively each of them occurs. The J_c was found to increase when the volume fraction of 2223 phase increases, suggesting the importance of the connectivity among 2223 grains. The J_c also increased with decreasing amount of residual carbon. The temperature and magnetic field dependences of J_c indicated characteristics of Josephson currents through superconducting–normal–superconducting barriers. After a discussion based on the alternative current limiting mechanisms proposed up to now, it is suggested that the homophase grain boundary limits the J_c. © *1996 American Institute of Physics.* [S0021-8979(96)02610-3]

I. INTRODUCTION

When silver-sheathed Bi2223 tapes are prepared by means of the powder-in-tube method, the oxide layer is usually comprised of aligned fine superconducting polycrystals together with several nonsuperconducting (non-SC) phases. In such a complicated fine structure, there are many factors influencing the J_c and a hierarchy might exist among them, where the most effective factor to dominate J_c depends on its prevalence.

Up to now, two models have been well known on the microstructural mechanism limiting J_c. One of them is the so-called "brick-wall" (BW) model.[1] It is essential that the current flowing in the c direction controls the J_c. The recent Umezawa *et al.* model[2] could be classified in the same category. The J_c is controlled by residual layers of 2212 phase at (001) twist boundaries of 2223 phase within grain colonies below a kink temperature (~80 K). Above the kink temperature, the grain-to-grain connections for boundaries containing 2212 are only proximity coupled and the connections are easily broken.

The second one is the "railway-switch" (RS) model proposed by Hensel *et al.*:[3] J_c is limited by $a-b$ plane transport and is controlled by grain-to-grain contact across low-angle colony boundaries. It might be suggested that a variety of coupling strengths exist for different misorientation angles similar to the case of YBCO.[4] Recently, Le Lay *et al.*[5] suggested that the pair breaking at the grain boundaries determines J_c from the model based on the superconducting–normal–superconducting (SNS) junctions. The grain boundaries are classified into two types. One is homophase boundaries, where two adjacent grains connect with various misorientation angles and impurities tend to segregate. The other is heterophase grain boundaries with the second phase like 2212, non-SC, and amorphous phases.

From the microstructural viewpoint, several other inhomogeneous factors such as sausaging, voids, microcracks, dispersion of non-SC phases, and so on have been reported as influencing the J_c.[6] In the present study, the microstructure dependence of J_c as well as the temperature and magnetic-field dependences have been investigated in detail in order to make clear the mechanism suppressing J_c.

II. EXPERIMENTAL PROCEDURE

High-purity oxide powders of Bi_2O_3, PbO, $SrCO_3$, $CaCO_3$, and CuO were weighed with a given composition ratio. The chemical compositions employed here are listed in Table I. The powders were mixed and calcined at 1073 K for 72 ks and ground again and then finally calcined at 1073 K for 72 ks. The powder was sheathed in silver tube with 6 mm outer diameter and cold worked by the groove roller to get a thin wire with about 1 mm diam. The thin wire was pressed into tape form with typical thickness less than 100 μm and heat treated under precise temperature control within 1 K. This thermomechanical treatment (TMT) process was repeated two times. Finally, short samples with 30 mm length were prepared. In order to investigate the influence of final heat treatment, the time and temperature were changed as listed in Table I.

In order to investigate microstructural changes, x-ray diffraction (XRD), scanning electron microscope (SEM), and electron microprobe analyses (EPMA) were carried out. As the XRD profile consisted of Bragg diffractions from several phases, all peaks were assigned by comparison with reference data except the 3:5 phase. By EPMA, two-dimensional mapping of characteristic x-ray intensities was measured and the area occupied by individual phases has been specified, where the 3:5 phase could be detected. The volume fraction of constituent phases was assessed from the intensity ratio of XRD peaks and corrected by the area ratio in scanning electron microscopy (SEM) image. It should be noted that the

[a]Electronic mail: osamura@hightc.mtl.kyoto-u.ac.jp

 0021-8979/96/79(10)/7877/6/$10.00

TABLE I. Chemical composition of the specimens used here, where all the specimens were heat treated in air.

Specimen number	Chemical composition Bi	Pb	Sr	Ca	Cu	TMT condition T (K)/t (ks)	Volume fraction (%) 2223	2212	2201	CP	CuO	2:1	3:5	J_c (A/cm^2) at 77 K
A1	1.6	0.4	1.6	2.0	2.8	1105/540	51	27	0	9	5	0	8	4 800
A2	1.6	0.4	1.6	2.0	2.8	1108/540	78	7	0	6	7	0	2	7 200
A3	1.6	0.4	1.6	2.0	2.8	1109/540	90	1	0	3	4	0	2	9 700
A4	1.6	0.4	1.6	2.0	2.8	1110/540	89	0.5	0	4	4	0	2.5	6 400
A5	1.6	0.4	1.6	2.0	2.8	1112/540	80	7	0	6	3	0	4	5 200
A6	1.6	0.4	1.6	2.0	2.8	1113/540	65	17	5	0	3	0	10	3 600
B1	1.6	0.4	1.6	2.0	2.8	1109/720	83	8	0	4	3	0	2	5 900
B2	1.6	0.4	1.6	2.0	2.8	1109/720	86	5	0	4	3	0	2	6 200
B3	1.6	0.4	1.6	2.0	2.8	1109/720	87	5	0	3	3	0	2	11 700
B4	1.6	0.4	1.6	2.0	2.8	1109/720	88	6	0	3	2	0	2	15 700
C1	1.6	0.4	1.6	2.0	2.8	1109/720	83	2	0	7	6	0	2	4 500
C2	1.6	0.4	1.7	1.9	2.8	1109/720	79	9	2	7	2	0	1	2 850
C3	1.6	0.4	1.8	1.8	2.8	1109/720	38	30	3	5	5	0	19	900
C4	1.7	0.3	1.6	2.0	2.8	1109/720	80	12	2	2	2	2	0	2 100
C5	1.7	0.3	1.7	1.9	2.8	1109/720	81	12	0	3	1	1	2	4 300
C6	1.7	0.3	1.8	1.8	2.8	1109/720	80	14	2	1	1	0	2	2 800
C7	1.8	0.2	1.6	2.0	2.8	1109/720	51	29	4	5	2	9	0	750
C8	1.8	0.2	1.7	1.9	2.8	1109/720	79	11	3	2	2	3	0	1 550
C9	1.8	0.2	1.8	1.8	2.8	1109/720	61	30	2	3	2	0	2	800

volume fraction determined here, however, was not strictly quantitative, but semiquantitative. The carbon was analyzed by using an ordinary oxygen-combustion–infrared-absorption (LECO) technique.

The critical current measurements were performed at 77 and 4.2 K with criterion of 1 μV/cm. The critical current density J_c was defined as the critical current divided by the cross-sectional area of oxide layer.

III. EXPERIMENTAL RESULTS

A. Microstructure dependence of J_c

Table I is a summary of the microstructural analysis for a part of specimens investigated here. Seven phases have been detected for those specimens; two superconducting phases at 77 K, and 2201, Ca_2PbO_4, CuO, and Bi-free 2:1 and 3:5 phases as the detailed information indicates in Table II. The heat treatment temperature was varied for the A series specimen. Comparing these specimens, high J_c was found to be obtainable in the so-narrow temperature region between 1105 and 1115 K and the highest value is achieved at 1109 K.[7] Here, six phases were detected as listed in Table I. CuO and 3:5 phase increased with decreasing temperature. 2212 and CP phases became minimum at intermediate temperatures, while the volume fraction of the 2223 phase became maximum. Several specimens were prepared with the same conditions indicated as B series. Their J_c together with a variation of constituted phases is markedly scattered. For the C series specimens, the chemical composition was changed under the same TMT condition, where in total seven phases could be detected, but the maximum number was six in each specimen as discussed elsewhere.[7]

TABLE II. Oxide phases detected in the present article where ○ indicates an easy identification. △ a necessity of precise measurement, and × an overlapping by the major 2223 phase.

	Phase	Detected by X ray	Detected by EPMA	Present symbol	Usual symbol
SC	$(Bi,Pb)_2Sr_2Ca_2Cu_3O_z$	○	△	2223	243
Phase	$Bi_2Sr_2CaCu_2O_z$	○	△	2212	232
	$Bi_2Sr_2CuO_z$	○	○	2201	221
Non-SC	$(Sr,Ca)_2CuO_3$	○	○	2:1	0.21, 2:1AEC
	$(Sr,Ca)CuO_3$	○	○	1:1	011
Phase	$(Sr,Ca)_3Cu_5O_3$	×	○	3:5	0.35, 14:24AEC
	CuO	○	○	CuO	001
	Ca_2PbO_4	○	○	CP	

The influence of microstructure on J_c has been examined. In principle, the existence of non-SC phases forces J_c to decrease, because of reducing the volume fraction of SC phase. Figure 1 shows the change of transport critical current density as a function of total amount of non-SC phases, which is the sum of (2201), CuO, CP, 2:1, and 3:5 phases. When the volume fraction was less than 15%, the correlation is found to be very poor between J_c and the total amount of non-SC phase.

The connection between Bi2223 superconducting grains themselves is necessary, because the coherence length is so short that the proximity effect is very weak. As shown in Fig. 2, the J_c increases with increasing volume fraction of Bi2223 phase. Beyond a value of 68%–74% Bi2223 phase, the J_c increases remarkably with the volume fraction of Bi2223 phase. This threshold value corresponds to the random percolation limit, indicating that the 2223 phase is disconnected by other non-SC phases below this fraction. When the volume fraction exceeds 90%, the J_c is expected to reach a remarkably high level. Figure 3(a) shows a typical microstructure of the homophase boundary connecting two 2223 grains with low misorientation angle. The intergrown 2212 layers have been often observed within the matrix as shown

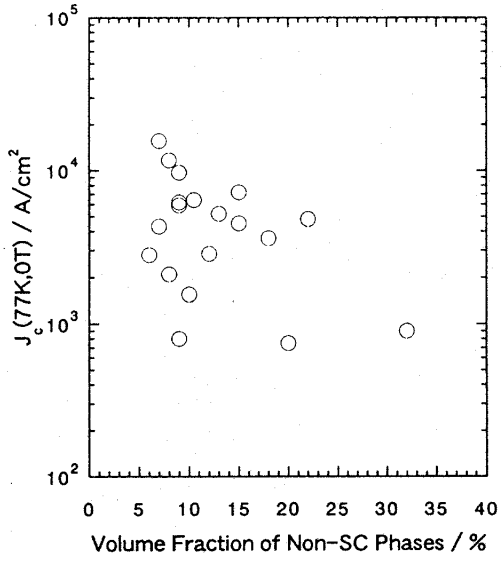

FIG. 1. Relation between the J_c at 77 K and the volume fraction of nonsuperconducting phases.

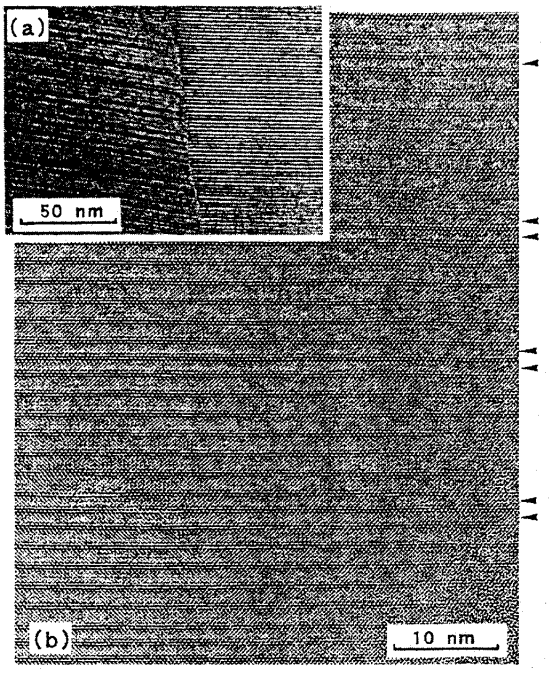

FIG. 3. (a) TEM microphotographs of the homophase boundary connecting two 2223 grains and (b) the lattice image of the right-hand-side grain, where the intergrown 2212 layers are indicated by arrows.

in Fig. 3(b). The twist boundaries including 2212 layers were rarely found in the present specimens.

In the present study, the amount of Bi2212 phase was accessed by using the diffraction technique. So the 2212 phase detected here is not the intergrown layers within the 2223 grain, but the second phase mostly at the heterophase grain boundary. Figure 4 shows the change of J_c as a function of 2212 volume fraction. The J_c tends to increase with decreasing the volume fraction of 2212 phase. The volume fraction dependency, however, is scattered below a volume fraction less than 10% and the J_c was not improved effectively by approaching the zero volume fraction of 2212 phase. This suggests that the J_c is dominated by another factor.

As reported previously by Flükiger *et al.*,[8] the J_c increases with decreasing carbon content. When the carbon content is high, the amorphous phase including carbon has been observed at the heterophase grain boundary. In the present specimens prepared with the same TMT condition, the carbon content was controlled by limiting the time for exposing the calcined powder in air. As shown in Fig. 5, the carbon content was changed from 0.7 to 0.22 mass %. The J_c was found clearly to increase with decreasing carbon content.

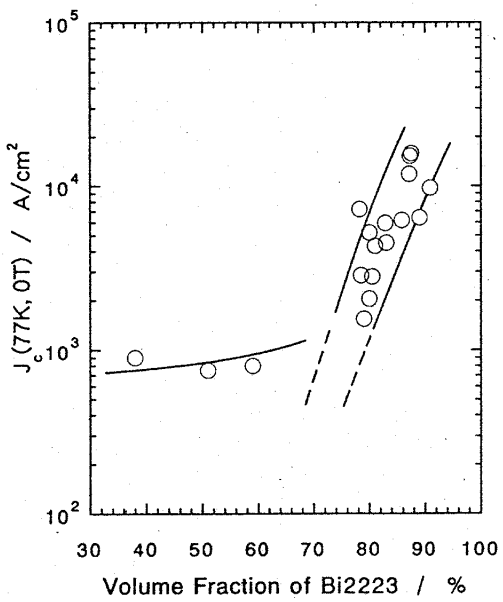

FIG. 2. Change of J_c as a function of volume fraction of Bi2223 phase.

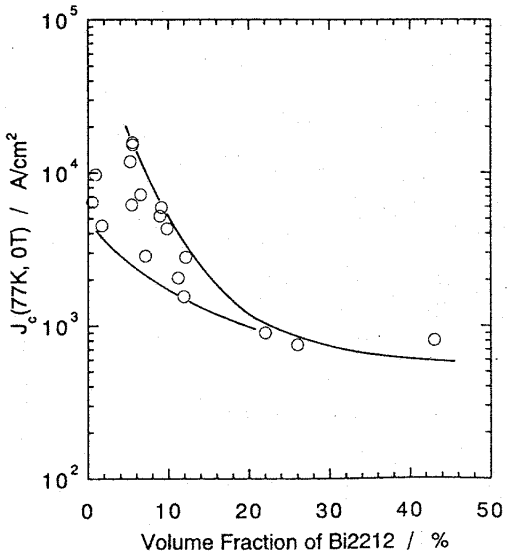

FIG. 4. Relation of the J_c at 77 K and the volume fraction of Bi2212 phase.

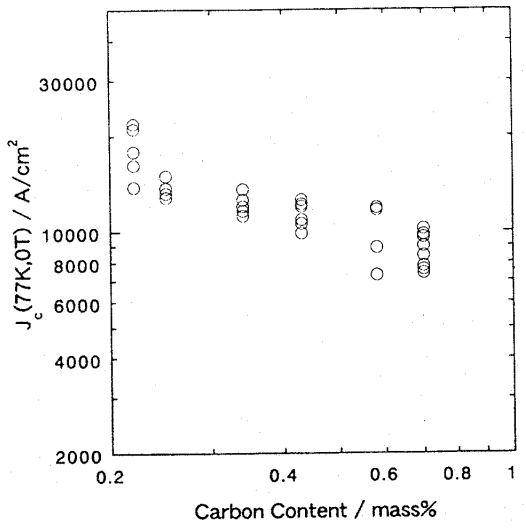

FIG. 5. Change of J_c at 77 K as a function of carbon content in the specimen.

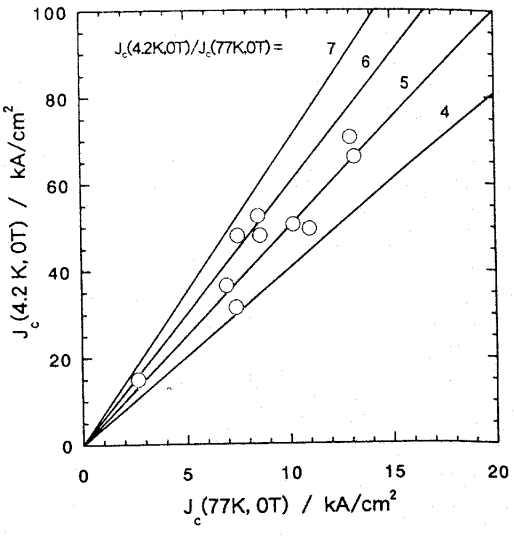

FIG. 7. Correlation of the J_c's measured at temperatures of 4.2 and 77 K, respectively.

B. Temperature and magnetic-field dependences of J_c

In order to specify the nature of the mechanism limiting the J_c, it is reasonable to investigate the transport behavior as a function of temperature as well as magnetic field. Figure 6 shows the field dependence of logarithmic critical current density. Its magnetic-field dependence could be separated into two parts depending on the field strength. A rapid decrease of J_c is observed, corresponding to so-called weak link phenomenon, in the low-magnetic-field region around the zero field. In the second region except the low-magnetic-field region, an exponential relationship holds over the entire range of magnetic field and temperature.

The zero-field J_c values at 77 and 4.2 K have been examined for many specimens as their correlation is indicated in Fig. 7. Their ratio is found to be lying in the range between 4 and 7. It seems that the temperature dependence of zero-field J_c values is self-consistent for all the specimens examined here. The critical current at zero field will be suggested to be limited by Josephson current as discussed in the following.

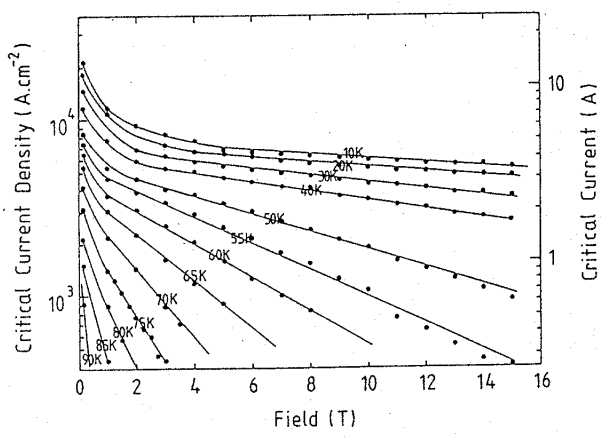

FIG. 6. Magnetic-field dependence of J_c at various temperatures, where the magnetic field was applied orthogonally to the specimen surface and the current flow.

The weak link behavior has been discussed for several high-temperature SC (HTSC) materials by many investigators. The temperature dependence of J_c at zero magnetic field can be analyzed using the theory by Ambegaoka and Baratoff,[9] where the Josephson current at zero magnetic field is given by the equation

$$\frac{I_c(T)}{I_c(0)} = \left(1 + \frac{b}{R_n(0)}\frac{T}{T_c}\right)\frac{\Delta(T)}{\Delta(0)}\tanh\frac{\Delta(T)}{2kT}, \tag{1}$$

where b, $R_n(0)$ are the constant and $\Delta(0)$ is the gap energy at zero temperature in the framework of BCS theory. Its temperature dependence is expressed as

$$\Delta(T) = 1.82\left(1 - \frac{T}{T_c}\right)^{1/2}\Delta(0). \tag{2}$$

The temperature dependence of Eq. (1) is evaluated numerically by changing the parameter $b/R_n(0)$ as shown by the solid curves in Fig. 8. From the experimental data indicated in Fig. 6, the zero field value is plotted as a function of reduced temperature as superimposed in Fig. 8. Comparing with the theoretical values, the parameter $b/R_n(0)$ has been deduced to be 1.5 to 3. The corresponding value of I_c(4.2 K)/I_c(77 K) becomes 4–6, when the critical temperature is 104 K.

As shown in Fig. 6, the linear dependence of logarithmic J_c with magnetic field has been observed for the present specimens. According to a model based on pair breaking through SNS junctions by Le Lay *et al.*,[5] the critical current has an exponential functional form given by

$$J_c(B,T) = \alpha(T)\exp\left(-\frac{\mu_0 H}{\beta(T)}\right), \tag{3}$$

where the applied field is orthogonal to the direction of current flow, $\alpha(T)$ is a function of temperature alone and $\beta(T)$

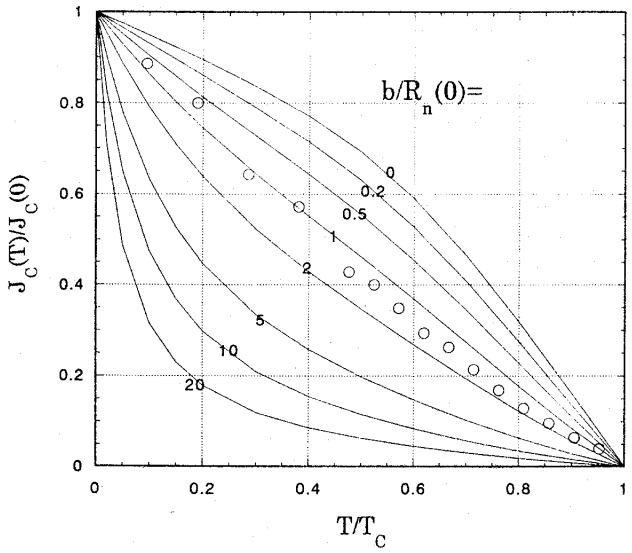

FIG. 8. The normalized critical current density as a function of reduced temperature, where the open circles are experimental data.

is inversely proportional to the electron scattering length in the normal barrier, and the width of the barrier as given by the equation

$$\beta(T)=\hbar/(2\sqrt{3}eld), \tag{4}$$

where e is the electronic charge, l is the electron scattering length in the normal barrier, and d is the width of the barrier. As shown in Fig. 6, the logarithmic critical current density is linearly changing in most of the magnetic field range. The β was found to decrease with increasing temperature. As discussed by Le Lay *et al.*, the exponential dependence is understood as a result from considering quantum-mechanical tunneling through a barrier. They also suggested that the grain boundaries are the most obvious microstructural feature in the present tape that could act as a tunneling barrier to superelectrons as discussed later.

IV. DISCUSSION

When there are several factors limiting the current, a hierarchy is suggested among them. The importance of their factors depends in practice on the level of critical current density. When the prevalence of the most effective factor is diminished, then subsequent candidates appear to control the J_c. With respect to this hierarchy, Umezawa *et al.*[2] have suggested that the first limit to the current is provided by the c-direction path at the (001) twist boundaries including 2212 layers which separate the grains within a colony. At temperatures below 80 K, these 2212 layers are superconducting at low magnetic fields. Therefore the c-axis supercurrent transport is important in polycrystalline Bi2223 tapes, at least until the superconducting c-axis connection is destroyed above a specific temperature $T'(H)$. They concluded, therefore, that remaining layers of 2212-BSCCO at (001) twist boundaries provide a widespread current-limiting mechanism in Ag-sheathed Bi2223 tapes having J_c(77 K, 0 T) values up to at least 20 000 A/cm^2. In the present specimens, however, the feature of the transport current at 77 K is characterized in terms of Josephson current in the low-magnetic-field region. This observation does not fit with the suggestion of Umezawa *et al.*

The present investigation has made clear several correlations between the J_c and microstructure. One of them is the dependence on the total amount of non-SC phases. As shown in Fig. 1, it is clear that the decreasing total amount does not give any direct correspondence with increasing J_c. There are two types of 2212 phase in the present specimens: the intergrown 2212 embedded in 2223 phase and the well-separated 2212 phase neighboring with 2223 phase. The former is detected by TEM, but could not be quantitatively assessed in the present experiment. The latter volume fraction was determined by means of XRD and EPMA. The decreasing volume fraction of the 2212 phase is possibly linked to the increase of homophase grain-boundary area. As shown in Fig. 4, the volume fraction dependence of J_c, however, becomes obscure in the region less than 10%. This suggests that the J_c will be dominated by other factors at least in this region. As shown in Fig. 5, the decrease of carbon content correlates strongly with the increase of J_c. There is no inconsistency when we assume the increase of clean homophase grain boundary by decreasing the reduced carbon content.

A clear correlation has been found between J_c and the 2223 volume fraction as shown in Fig. 2. Beyond a threshold value, the J_c increases remarkably with the volume fraction of 2223 phase. The threshold is known theoretically to appear at 64%–75% in the random percolation limit and 78%–84% in the correlated percolation one.[10] This indicates that the 2223 phase is disconnected by other non-SC phases when the volume fraction of 2223 phases is less than the percolation limit. As shown in Fig. 2, the threshold seems to be described in terms of the random percolation limit.

There is still macroscopic inhomogeneity for the Bi2223 tapes. At the interface region with the silver sheath, the 2223 grains are often observed to be longer and better aligned than those in the center of tape. According to the recent magneto-optical measurements,[11] the supercurrents concentrate well at this interface region. It becomes important to analyze in detail these well-aligned regions of Bi2223 grains. Perhaps, even though Bi2223 layered grains have a comparatively good overall alignment, they connect each other with various misorientation angles. As reported by Dimos *et al.*,[4] the interface J_c changes depending on different misorientation angle in the YBCO system, but, at present, such a quantitative relationship has been not yet made clear for the present Bi2223 system. As shown in Fig. 2, the high volume fraction exceeding 90% corresponds to the high J_c value. This fact strongly suggests that the area of low-angle homophase grain boundary increases and as a result the concentration of segregated impurities such as carbon is diluted at the grain-boundary region.

The present magnetic-field dependence of J_c supports the phenomenological pair breaking SNS model as discussed by Le Lay *et al.*[5] The parameter β given in Eq. (4) was found to decrease with increasing temperature. It depends theoretically on the electron scattering length and the barrier width. When the temperature increases, the scattering length should

decrease in a clean normal barrier. On the other hand, the barrier width tends to increase with increasing temperature, because of degradation of superconductivity, that is, lowering of critical temperature will occur continuously as a function of position from the grain boundary. The width of normal barrier at the grain boundary is suggested to increase with increasing temperature. Therefore, the decrease of $\beta(T)$ might be explained in terms of the increasing barrier width with increasing temperature.

Finally, as a summary of the discussion mentioned above, it is concluded that the present observation fits with RS model, where J_c is limited by $a-b$ plane transport and is controlled by the low-angle homophase boundaries.

V. CONCLUSION

In the present study, the microstructural aspect influencing the J_c has been mainly investigated as summarized in the following. There are many microstructural factors limiting J_c in practice. In a hierarchy among them, however, the most effective factor to dominate J_c depends on how extensively each of them occurs. For the present specimens with J_c values less than 20 000 A/cm^2, the J_c increased with increasing volume fraction of 2223 phase and with decreasing amount of residual carbon. The temperature and magnetic-field dependences indicated characteristics of Josephson current through SNS barriers. The experimental evidence is not inconsistent with the suggestion that the homophase grain boundary between Bi2223 grains controls the J_c.

ACKNOWLEDGMENTS

The authors express their hearty thanks to Professor K. Watanabe of the High Magnetic Field Center for Superconducting Materials at Tohoku University for his help in the critical current measurements. One of us (K.O.) his gratitude to the Ministry of Education, Science, and Culture of Japan for the Scientific Research Grant-in-Aid (Project No. 06555204).

[1] L. Bulaevskii, J. R. Clem, L. I. Glazman, and A. P. Malozemoff, Phys. Rev. B **45**, 2545 (1992).

[2] A. Umezawa, Y. Feng, H. S. Edelman, Y. H. High, D. C. Larbalestier, Y. S. Sung, E. E. Hellstrom, and S. Fleshler, Physica C **198**, 261 (1992).

[3] B. Hensel, J.-C. Grrivel, A. Jeremie, A. Perin, A. Pollini, and R. Flükiger, Physica C **205**, 329 (1993).

[4] D. Dimos, P. Chaudhari, J. Mannhardt, and F. K. LeGouses, Phys. Rev. Lett. **61**, 219 (1988).

[5] L. Le Lay, C. M. Friend, T. Maruyama, K. Osamura, and D. P. Hampshire, J. Phys. Condensed Matt. **6**, 10 063 (1994).

[6] K. Osamura, in *Proceedings of the 2nd Pacific Rim International Conference on Advanced Materials and Processes*, edited by K. S. Shin *et al.* (KIMM, 1995), p. 1937.

[7] K. Osamura, S. Nonaka, and M. Matsui, Physica C **257**, 79 (1996).

[8] R. Flükiger, B. Hensel, A. Pollini, J. C. Grivel, A. Perin, and A. Jeremie, *Advances in Superconductivity V* (Springer, Berlin, 1993), pp. 17–22.

[9] V. Ambegaoka and A. Baratoff, Phys. Rev. Lett. **10**, 486 (1963); **11**, 104 (1963).

[10] D. Stauffer, *An Introduction to Percolation Theory* (Taylor and Francis, London, 1988).

[11] D. C. Larbalestier *et al.*, in The 1995 International Workshop on Superconductivity cosponsored by ISTEC and MRS, Hawaii, June, 1995, p. 17.